

## Optical and electrical transport measurements on amorphous mixtures of Cs and Sb

R. D. Swenumson\* and U. Even

*Chemistry Department, Tel-Aviv University, Tel-Aviv, Israel*

(Received 21 November 1980)

Optical and electrical transport properties were investigated in amorphous Cs-Sb mixtures at 6 K. A metal-nonmetal transition is observed as a function of Cs atomic fraction ( $X$ ) and both the transport and optical properties indicate that this occurs at  $X = 0.68$ . The dc conductivity at this composition is  $\sim 150 \Omega^{-1} \text{cm}^{-1}$  which is consistent with acceptable values of Mott's minimum metallic conductivity. The mixtures can be partitioned into three distinct composition regions: (1)  $X < 0.64$ , in which the mixtures are semiconducting; (2)  $0.64 < X < 0.68$ , in which the states near the Fermi energy apparently are localized; and (3)  $X > 0.68$ , in which the mixtures are metallic. The optical data indicate that within the broad composition range  $0.7 < X < 0.95$ , approximately 1.6 electrons are removed from the metallic conduction band for each Sb atom added to the system. Electrical transport data in Cs-Sb liquid alloys are compared with the present data in the amorphous solid state.

### I. INTRODUCTION AND EXPERIMENT

The metal-nonmetal transition (MNMT) is a field which has inspired considerable activity over the last twenty years.<sup>1-8</sup> Particularly good accounts of the developments in the field are contained in Refs. 1 and 2. Reported here are the results of an investigation of amorphous solid Cs-Sb mixtures. Electrical transport and optical data are presented and discussed in relation to the MNMT which occurs in this system at 6 K as the composition is changed. The influence of the chemical bond on the physical properties of these mixtures is examined. A comparison is made between these and the high-temperature (800°C) liquid Cs-Sb mixtures which also exhibit an MNMT.<sup>9,10</sup>

All measurements were performed under ultrahigh vacuum (UHV) conditions ( $10^{-9}$  Torr). The Cs-Sb mixtures were prepared by coevaporation of each component from separate effusive sources. The Cs source<sup>11</sup> is a resistively heated reflux-type oven which collimates the beam with a series of cold baffles. Capillary action returns the Cs which is stopped by the baffles to the hot part of the Cs source. The Sb source is a resistively heated alumina crucible. Molybdenum heat shields surround the source in order to reduce the power requirement ( $\sim 15$  W) at the routine operating temperature of 400°C. A quartz-crystal thickness gauge positioned near the sample substrate measured the deposition rates from the temperature-stabilized beam sources. The stability of each beam intensity is about 1%,

which implies a Cs-Sb mixture composition uniformity of 1%. The absolute deposition rate of each component (i.e., the composition) was determined by two independent means in the case of the Sb rate and by three independent methods in the case of the Cs rate. These methods are described elsewhere.<sup>12</sup> The materials Cs (99.98% pure) and Sb (99.9999% pure) were obtained from Koch-Light Laboratories, Ltd.

The sample substrate is a circular 1-in. sapphire window which is attached to a bath-type He cryostat. Technical details concerning the vacuum system, cryogenics, optics which spanned the energy range 0.65–5.5 eV, electrical transport measurements, and the construction and operation of the experimental system are found in Ref. 12.

### II. RESULTS

The dc conductivity of Cs-Sb amorphous mixtures appears in Fig. 1. Experimental values span approximately seven orders of magnitude from the pure Cs sample to mixtures near the stoichiometry  $\text{Cs}_3\text{Sb}_2$ . Within the composition range ( $X = \text{Cs}$  at fraction)  $0.7 < X < 1$  the conductivity varies relatively slowly with a slope of approximately 1 order of magnitude per 15 at. % change. The slope increases dramatically in the range  $0.62 < X < 0.64$  to over 2 orders of magnitude per 1 at. % change. Conductivities for compositions  $X < 0.62$  were not measureable since they extended beyond the experimental measurement range. Unlike pure Sb at

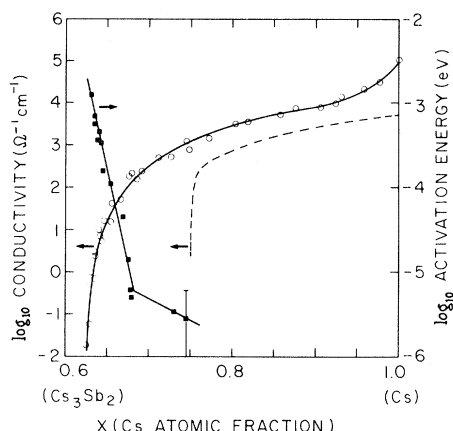


FIG. 1. The composition dependence of the dc conductivity (O) and the activation energy (■) of amorphous Cs-Sb mixtures at 6 K and the dc conductivity of liquid Cs-Sb alloys (— — —) at 800 °C.

800 °C, at 6 K the conductivity of Sb lies many orders of magnitude below the lowest conductivity shown in Fig. 1.<sup>13</sup> This is a consequence of the semimetallic character of Sb.

In the temperature range 5.5–13 K the conductivity of Cs-Sb mixtures was found to fit the functional form  $\exp(\text{const } T^\alpha)$  where  $\alpha = -1.0 \pm 0.2$  for compositions  $X < 0.64$ . The activation energy associated with this semiconductor-like temperature dependence appears in Fig. 1. Two distinct regions of composition dependence are apparent in the data. The composition range  $0.63 < X < 0.68$  has a much greater composition dependence than the range  $X > 0.68$ . In the former range the activation energy decreases by over two orders of magnitude from 1 meV to 5  $\mu\text{eV}$  with increasing  $X$ . The error in determining the activation energy is roughly the size of the symbols in the graph except in the region  $0.64 < X < 0.68$  in which the nature of the temperature dependence changes from  $\alpha = -1.1 \pm 0.1$  at  $X = 0.64$  to  $-0.73 \pm 0.1$  at  $X = 0.643$ ,  $-0.40 \pm 0.15$  at  $X = 0.646$ ,  $-0.36 \pm 0.3$  at  $X = 0.654$ , and finally to the region  $X > 0.67$  in which the data are best described by a temperature coefficient of conductivity ( $\beta$ ) =  $d(\log_{10}\sigma)/dT$ . A wide range of compositions between 0.68 and 0.95 over which the temperature dependence is very small and the signal-to-noise ratio is low, results in a large error in the determination of the composition at which the temperature coefficient changes sign ( $X = 0.76 \pm 0.07$ ). The temperature coefficient of conductivity of pure Cs at 6 K is  $-8 \times 10^{-3} \text{ K}^{-1}$ . The conductivity is reversible ( $\pm 3\%$ ) in temperature up to 13 K at all compositions and in some

samples up to 20 K.

The optical-transmittance data were analyzed in order to obtain the optical constants by using a classical multiple-oscillator model.<sup>14</sup> The strength, frequency, and width of two to four oscillators plus the high-frequency dielectric constant were parameters which were iteratively adjusted by computer in order to minimize a certain error function. The error function characterized the quality of the fit of the transmittance predicted by the model to the optical-transmittance data. The averaged relative error across the entire energy range examined for each sample was less than 5%. A more detailed description of the data analysis is found in Ref. 12.

The real part of the dielectric constant  $\epsilon_1(E)$  is shown in Fig. 2. Beginning with pure Cs (curve A) for which  $\epsilon_1$  is less than zero below a certain photon energy, the curves progress monotonically to the composition  $X = 0.605$  (curve K). For all compositions the energy dependence of  $\epsilon_1$  is weak where  $E > 3 \text{ eV}$ . At low photon energy and for the compositions for which  $\epsilon_1$  is negative,  $\epsilon_1$  has a relatively strong energy dependence (Drude tail).

Shown in Fig. 3 is the optical conductivity of several mixtures whose compositions range from pure Cs to pure Sb. A broad maximum at 3 eV characterizes the pure Sb sample while a relatively narrow maximum occurs in the pure Cs sample at 1.2 eV. At high energy the intermediate composi-

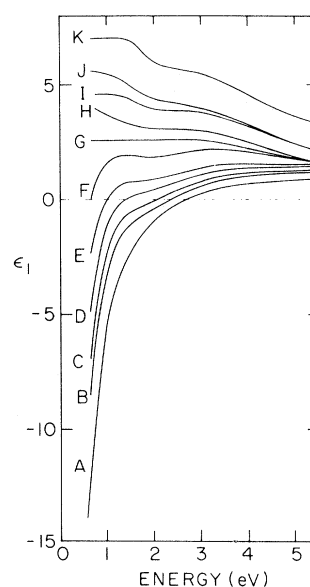


FIG. 2. The real part of the dielectric constant  $\epsilon_1$  vs energy for several compositions. A:  $X = 1.000$ , B: 0.945, C: 0.905, D: 0.825, E: 0.770, F: 0.708, G: 0.670, H: 0.646, I: 0.642, J: 0.630, K: 0.605.

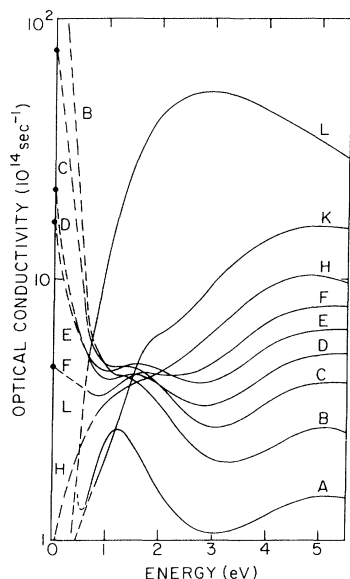


FIG. 3. The optical conductivity  $\sigma$  vs energy for several compositions. A:  $X = 1.000$ , B: 0.945, C: 0.905, D: 0.825, E: 0.770, F: 0.708, H: 0.646, K: 0.605, L: 0.000.

tions exhibit a monotonic increase of the optical conductivity with increasing  $X$ . At low energies the 1.2-eV feature associated with pure Cs persists to  $X = 0.605$ . The lower-energy limit of the present optical setup (0.65 eV) does not extend to sufficiently low energies to permit the observation of the turnaround of  $\epsilon_1$  for a pure Cs sample (— —) measured by other groups.<sup>15,16</sup> The other dashed lines represent extrapolations of the optical data to the dc conductivity values indicated at  $E = 0$ . This extrapolation serves as a quality check on the data-fitting procedure.

Figure 4 contains the low-energy (0.65 eV) values of  $\epsilon_1$  as a function of composition. A monotonic decrease of  $\epsilon_1$  from the positive values at  $X \sim 0.6$  to the negative values occurs with the largest composition dependence appearing in the range  $0.95 < X < 1$ .

A plasma frequency  $\omega_p$  can be deduced from the optical data assuming a nearly-free-electron model of the form<sup>17</sup>

$$\epsilon_1(\omega) = \epsilon_1(\infty) - (\omega_p/\omega)^2 + \epsilon_i(\omega), \quad (1)$$

where  $\epsilon_1(\infty) = 1 +$  the high-energy (core) polarization,  $\omega_p^2 = 4\pi ne^2/m^*$ ,  $n =$  the free-electron density,  $m^* =$  the effective mass, and  $\epsilon_i$  is a term correcting for interband transitions. If  $\epsilon_i$  can be neglected then the square root of the slope of a plot of  $\epsilon_1$  vs  $-E^{-2}$  is the plasma frequency in energy

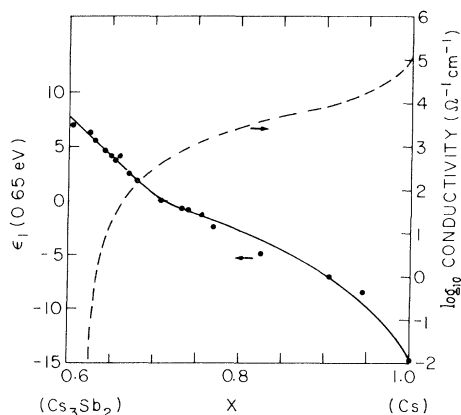


FIG. 4. The composition dependence of the real part of the dielectric constant  $\epsilon_1$  at 0.65 eV ( $\bullet$ ) and dc conductivity (— —) of Cs-Sb solid mixtures.

units. In the energy region  $\omega \ll \omega_p$ , the term  $\epsilon_i$  is a small correction in Cs and is of the order of 10%.<sup>16</sup> Based upon this model the plasma frequencies were determined for several metallic samples and normalized by  $\omega_p(X = 1)$ . The squares of these values are plotted in Fig. 5. Recent optical measurements on amorphous Cs-Xe mixtures<sup>18</sup> indicate that a significant difference exist between  $\omega_p$  in polycrystalline Cs (Refs. 15, 16, 19) and the value in amorphous Cs whose disordered structure may be stabilized by the addition of 5 at. % Xe. The value appropriate for amorphous Cs ( $\blacktriangle$ ) is plotted in Fig. 5.

Mixture densities used throughout this analysis were obtained by assuming that the samples consist of an amorphous alloy of hard spheres with a characteristic packing fraction of 0.45,<sup>20</sup> where the hard-sphere radius was obtained from crystalline densities and packing fractions. Corroborative evidence of the amorphous structure is the irreversible

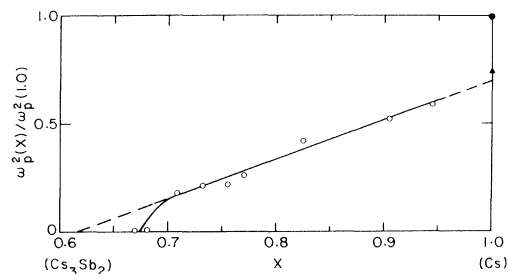


FIG. 5. The composition dependence of the square of the plasma frequency  $\omega_p^2(X)$  normalized by  $\omega_p^2(1)$  for Cs-Sb solid mixtures ( $\circ$ ), a pure Cs sample ( $\bullet$ ) deposited on a substrate at 6 K, and an amorphous Cs sample ( $\blacktriangle$ ) (see text).

increase in the dc conductivity after thermal cycling to temperatures above 15–20 K, which indicates that a more dense mixture results after the thermal cycling. A cursory examination of Fig. 1 reveals that the trends of conductivity versus  $X$  near  $X = 1$  are different for the solid and liquid (amorphous) mixtures. The rapid rise in conductivity as the pure Cs composition is approached is consistent with a structural change from the amorphous solid mixtures ( $X < 0.9$ ) to the more dense polycrystalline<sup>18</sup> structure of Cs. Analogous behavior is seen in other Cs-based solid mixtures.<sup>12,18</sup>

### III. DISCUSSION

Of primary importance to the task of comparing the present data on solid mixtures of Cs-Sb to the liquid-alloy data is to understand the influence of the different conditions under which each is studied. Furthermore it is desirable to minimize the differences in conditions when possible. One important factor is the structure. The preparation of amorphous mixtures by codeposition onto a cold substrate reduces the structural difference between this system and the liquid alloys (via the absence of long-range order).

The conductivity of liquid Cs-Sb (Ref. 9) is shown in Fig. 1 (— —). Most striking is the abrupt decrease in the conductivity with decreasing Cs content, which reaches a minimum at the stoichiometry Cs<sub>3</sub>Sb ( $X = 0.75$ ). No evidence of this compound forming in the solid mixtures is apparent from our conductivity data. Thus a major difference exists between the liquid and amorphous-solid data with respect to the nature of the chemical bond which determines compound formation.

One model of the MNMT is that of continuous classical percolation.<sup>8,21,22</sup> This theory as it relates to this discussion is presented in Ref. 18 in this issue. Numerical simulations<sup>23</sup> of classical percolation provide a critical exponent  $b = 1.6 \pm 0.1$  for the divergence of the conductivity at  $C^*$ ,  $\sigma \propto (C - C^*)^b$ . In order to test the applicability of percolation theory<sup>18</sup> to the Cs-Sb amorphous mixtures, a model was proposed in which the compound Cs<sub>3</sub>Sb<sub>2</sub> was assumed to be the insulating material and the excess Cs the metallic component. The metallic volume fraction scale  $C$  was determined from the hard-sphere packing model mentioned in Sec. II. The conductivity was fit to the functional form  $\sigma \propto (C - C^*)^b$  and replotted in Fig. 6 where the best-fit parameters ( $C^* = 0.083$  and  $b = 2.77$ ) defined the solid line through the

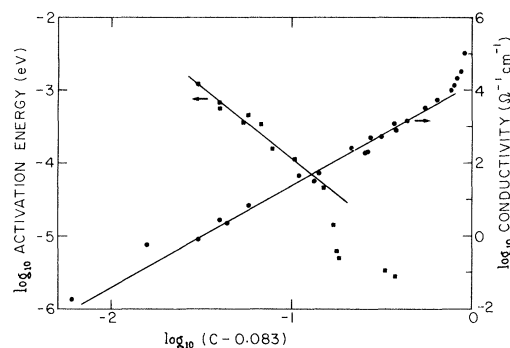


FIG. 6. The dc conductivity (●) and activation energy (■) vs  $C - 0.083$  ( $C =$  metallic volume fraction) of Cs-Sb solid mixtures. The slope of the solid line through the conductivity is 2.77 and that through the activation energy is  $-1.95$ .

conductivity data. For completeness the activation energy is plotted on the same scale and fit to the second straight line with a slope  $-1.95$ . The positive sign of the temperature coefficient of conductivity near  $C^*$  is in conflict with the negative sign expected from percolation theory. Other model materials based upon different compounds as the insulating background (CsSb, for example), also resulted in best-fit values of  $C^*$  and  $b$  which were inappropriate for the theoretical model of continuous classical percolation which requires that  $C^* = 0.145$  and  $b = 1.6$ .<sup>18</sup> Therefore the percolation model is ruled out to describe amorphous-solid mixtures of Cs and Sb.

A second model of the MNMT is due primarily to Mott.<sup>1,24</sup> The basics of this model are described in Ref. 18. Mott argues that when the system is near the MNMT, a local minimum in the density of states (pseudogap) exists at the Fermi energy. Under certain conditions, depending primarily upon the state of the disorder in the system,<sup>25</sup> the states at the Fermi energy are localized and the electrical transport properties at low temperature are governed by hopping conduction between localized states (variable-range hopping). Mott predicts<sup>1</sup> the temperature ( $T$ ) dependence of the conductivity for such a mechanism to be a power law in  $T^{-0.25}$ . In the composition range  $0.64 < X < 0.68$  in which the power law  $T^\alpha$  for the conductivity is in transition from the  $\alpha = -1$  dependence, where  $X < 0.64$  to  $\alpha \sim 0$  where  $X > 0.67$ , Mott's  $\alpha = -0.25$  dependence lies within the confidence limits of the three mixtures in the range  $0.646 < X < 0.67$ .

As the system is moved away from the MNMT

on the nonmetallic side, the pseudogap widens and may eventually become a real gap in which a finite-energy range overlapping the Fermi energy exists and in which the density of states is zero. The system is then semiconductorlike and the temperature dependence of the conductivity is a power law in  $T^\alpha$ ,  $\alpha = -1$ . The temperature dependence of the amorphous Cs-Sb solids in the range 6–13 K obeys this power law with  $\alpha = -1.0 \pm 0.2$  in the composition range  $X < 0.64$ .

Within the Mott picture the conductivity data imply that a real gap (however small) exists and narrows with increasing  $X$  for compositions  $X > 0.64$ . For compositions  $X > 0.64$  a different mechanism appears whose temperature dependence is consistent with Mott's variable-range-hopping model, whereby the pseudogap is filled with localized states near the Fermi energy. At  $X = 0.68$  the composition dependence of the activation energy changes dramatically. The conductivity at this composition is  $\sim 150 \Omega^{-1} \text{cm}^{-1}$ . The composition endpoints associated with Mott's range of the minimum metallic conductivity ( $100\text{--}1000 \Omega^{-1} \text{cm}^{-1}$ ) are 0.67 and 0.74.

The MNMT is revealed clearly in the optical data (Fig. 2), where metallic character ( $\epsilon_1 < 0$  as  $E \rightarrow 0$ ) is displayed by curves  $A\text{--}E$  and nonmetallic character ( $\epsilon_1 > 0$  as  $E \rightarrow 0$ ) is seen in curves  $G\text{--}K$ . The location of the MNMT is at the composition where  $\epsilon_1(E = 0)$  changes sign. If a sufficiently low probe energy is used, an approximation to  $\epsilon_1(E = 0)$  can be made and the MNMT located at the composition where  $\epsilon_1(E \sim 0) = 0$ . Using the lowest photon energy in the present study (0.65 eV), this procedure locates the transition at  $X_T = 0.71$ . However, since this value of  $X_T$  will be shown to be somewhat large compared to the value indicated by other data, the criterion which sets an upper limit ( $\Delta E$ ) on the photon energy necessary to perform this analysis has not been met. That a small enough photon energy was not used to satisfy this criterion is inferred from Fig. 2. Curve  $F$  reveals that although the trend toward negative (metallic) values is present, a sufficiently low photon energy was not available to produce them, thereby indicating a spuriously high value of  $X_T$ .

The optical properties of a system which exhibits an MNMT of the Mott type<sup>1,24</sup> or of a variety of types described by other models,<sup>26–28</sup> have a characteristic discontinuity at the transition. A discontinuity is not apparent in Fig. 4, but a slight break in the composition dependence is noticeable at the zero crossing.

One method of extracting a gap energy from optical data of amorphous materials<sup>29</sup> is to extrapolate the low-energy dependence of the function  $\sqrt{\epsilon_2(E)}E$  to the energy axis, where  $\epsilon_2$  is the imaginary part of the dielectric function. The intercept ( $E_g$ ) is the gap energy. This analysis was performed on the amorphous Cs-Sb optical data with the result that very small gap energies (0–10 meV) occur for compositions  $X < 0.63$ . Because of the extrapolation procedure an error of 20 meV is present; however, the gap clearly had closed for  $X > 0.64$ . These gap energies are to be compared with the optical gap of the pure amorphous Sb sample which was determined to be  $260 \pm 20$  meV using the same procedure. The small values of  $E_g$  for compositions  $X < 0.64$  are consistent with the small semiconductor-type activation energies in Fig. 1, which provides supporting evidence that the gap in this composition region is a true gap and not a pseudogap filled with localized states.

In Sec. II it was shown that a plasma frequency ( $\omega_p$ ) can be assigned to each metallic sample. If we assume that  $m^*$  does not change radically with composition, then the free-electron density  $n$  is proportional to  $\omega_p^2$ . The normalized (see Sec. II) values of  $\omega_p^2$  appear in Fig. 5. The approximately linear trend in the composition range  $0.7 < X < 0.95$  suggests the simple picture that a constant number of free electrons are removed from the conduction band per unit decrease in  $X$ . The slope of the line in Fig. 5 indicates that for every Sb atom added to the system, approximately 1.6 free electrons are removed. A crude model suggests that the bonding mechanism (possibly covalent)<sup>9</sup> which is responsible for this behavior is related to the formation of the compound  $\text{Cs}_3\text{Sb}_2$ . Evidence of the  $\text{Cs}_3\text{Sb}_2$  compound formation is suggested by electrical-conductivity measurements in solid film mixtures prepared at  $100^\circ\text{C}$ .<sup>30</sup> The optical-conductivity data contained in Fig. 3 reveal that throughout the composition range  $0.6 < X < 1$  the 1.2-eV feature associated with pure Cs persists noticeably. If the simple model based upon the formation of the compound  $\text{Cs}_3\text{Sb}_2$  were responsible for the MNMT, an optical feature associated with Cs would not be expected to be present, *a priori*, unless the optical properties of the compound contain the feature as well. Thus, this simple model is not well founded.

The data point appropriate for amorphous Cs ( $\blacktriangle$ ) (Ref. 18) is included in Fig. 5. The proximity of the amorphous Cs data point to the extrapolation intercept of the solid line in Fig. 5 with  $X = 1$  gives indirect support to the assumption that the Cs-Sb

mixtures prepared during this study are amorphous.

The data departs from the linear trend between the compositions  $X = 0.69$  and  $0.7$ , and the free-electron density approaches zero at about  $X = 0.68$ . A different composition-dependent mechanism apparently interrupts the one which is responsible for the linear dependence in the range  $0.7 < X < 0.95$ . One possible mechanism is localization, whereby localized states begin to appear near the Fermi energy when  $X < 0.7$ . This supposition is consistent with the inferences which were drawn from the changing character of the activation energy in the region  $0.64 < X < 0.68$ .

#### IV. SUMMARY

Several points can be made which summarize the properties of Cs-Sb mixtures.

(a) The CsSb mixtures studied are amorphous as inferred from (i) the irreversibility of the conductivity to thermal cycling and (ii) the relative fit of the amorphous Cs optical data point compared to the polycrystalline Cs point in Fig. 5.

(b) The MNMT is a continuous transition as revealed by the electrical transport and optical properties.

(c) The model of continuous classical percolation is compatible neither with the conductivity nor with the temperature dependence of the conductivity of these mixtures.

(d) The optical data indicate that the MNMT is located at  $X = 0.68 \pm 0.01$ . An abrupt change in the composition dependence of the activation energy occurs at this same composition. The conductivity at  $X = 0.68$  is  $\sim 150 \Omega^{-1} \text{cm}^{-1}$ , which is a suitable value for Mott's minimum metallic conductivity.

(e) Mixtures for which  $X > 0.68$  exhibit metallic properties, and the temperature coefficient of conductivity is near zero ( $\pm 5.0 \times 10^{-4} \text{K}^{-1}$  for compositions  $0.68 < X < 0.95$ ).

(f) Mixtures for which  $X < 0.64$  are semiconducting. The optical properties and the temperature dependence of the conductivity indicate the presence of an optical gap.

(g) The nature of the mixtures within the narrow composition range  $0.64 < X < 0.68$  is not unambiguously defined, but it seems to be a transition region between the semiconducting range  $X < 0.64$  and the metallic range  $X > 0.68$  and associated with the filling of a pseudogap. Most of the data in this transition region are consistent with Mott's  $T^{-0.25}$  power law (within the statistical confidence limits of the data) and all of the data in this region exclude the  $T^{-1}$  (semiconducting) power law.

(h) The nature of the chemical bond in amorphous solid Cs-Sb mixtures is significantly different from that in the liquid alloys. The compound  $\text{Cs}_3\text{Sb}$  which is strikingly evident in the liquid data<sup>9,10</sup> is not present in the amorphous solid.

(i) Approximately 1.6 electrons are removed from the metallic conduction band for each Sb atom added to mixtures in the composition range  $0.7 < X < 0.95$ . However, a simple model whereby 1.5 electrons are removed per Sb atom via the formation of the compound  $\text{Cs}_3\text{Sb}_2$  is not appropriate.

#### ACKNOWLEDGMENTS

This work was supported by the U. S.-Israel Binational Science Foundation and the Basic Research division of the Israel Academy of Science.

\*Present address: Bell Laboratories, 600 Mountain Ave., Murray Hill, N. J. 07974.

<sup>1</sup>N. F. Mott, *Metal-Insulator Transitions* (Taylor and Francis, London, 1974).

<sup>2</sup>*The Metal-Nonmetal Transition in Disordered Systems*, edited by L. R. Friedman and D. P. Tunstall (SUSSP, Edinburgh, 1978).

<sup>3</sup>U. Even and J. Jortner, *Philos. Mag.* **25**, 715 (1972).

<sup>4</sup>R. C. Cate, J. G. Wright, and N. E. Cusack, *Phys. Lett.* **32A**, 467 (1970).

<sup>5</sup>J. C. Thompson, *Electrons in Liquid Ammonia* (Clarendon, Oxford, 1976).

<sup>6</sup>F. Hensel, *Can. J. Chem.* **55**, 2225 (1977).

<sup>7</sup>R. D. Swenumson, U. Even, and J. C. Thompson, *Phi-*

*los. Mag.* **37**, 311 (1978).

<sup>8</sup>J. Jortner and M. H. Cohen, *Phys. Rev. B* **13**, 1548 (1976).

<sup>9</sup>W. Freyland and G. Steinleitner, in *Third International Conference on Liquid Metals*, edited by R. Evans and D. A. Greenwood (Institute of Physics, Bristol and London, 1977), p. 488.

<sup>10</sup>W. Freyland and G. Steinleitner, *Ber. Bunsenges. Phys. Chem.* **80**, 810 (1976).

<sup>11</sup>R. D. Swenumson and U. Even, *Rev. Sci. Instrum.* **52**, 559 (1981).

<sup>12</sup>R. D. Swenumson and U. Even, this issue, paper III.

<sup>13</sup>R. Avci and C. P. Flynn, *Phys. Rev. B* **19**, 5967 (1979).

- <sup>14</sup>H. W. Verleur, *J. Opt. Soc. Am.* 58, 1356 (1968).
- <sup>15</sup>U. S. Whang, E. T. Arakawa, and T. A. Callcott, *J. Opt. Soc. Am.* 61, 740 (1971).
- <sup>16</sup>N. V. Smith, *Phys. Rev. B* 2, 2840 (1970).
- <sup>17</sup>M. H. Cohen, *Philos. Mag.* 3, 762 (1958).
- <sup>18</sup>R. D. Swenumson and U. Even, this issue, paper I.
- <sup>19</sup>T. Hanyu and S. Yamaguchi, *J. Phys. Soc. Jpn.* 37, 994 (1974).
- <sup>20</sup>N. W. Ashcroft and J. Lekner, *Phys. Rev.* 145, 83 (1966).
- <sup>21</sup>S. Kirkpatrick, *Rev. Mod. Phys.* 45, 574 (1973).
- <sup>22</sup>I. Webman, J. Jortner, and M. H. Cohen, *Phys. Rev. B* 11, 2885 (1975).
- <sup>23</sup>S. Kirkpatrick, *Phys. Rev.* 27, 1722 (1971).
- <sup>24</sup>N. F. Mott, *Philos. Mag. B* 37, 377 (1978).
- <sup>25</sup>N. F. Mott, *Philos. Mag.* 13, 989 (1966).
- <sup>26</sup>J. C. Phillips, *Rev. Mod. Phys.* 42, 317 (1970).
- <sup>27</sup>I. Webman, J. Jortner, and M. H. Cohen, *Phys. Rev. B* 15, 5712 (1977).
- <sup>28</sup>J. C. Maxwell-Garnett, *Philos. Trans. Soc. London* 203, 385 (1904); and 205, 237 (1906).
- <sup>29</sup>M. L. Theye, in *Proceedings of the 5th International Conference on Amorphous and Liquid Semiconductors*, edited by J. Stuke and W. Brenig (Taylor and Francis, London, 1974), p. 479.
- <sup>30</sup>K. Miyake, *J. Appl. Phys.* 31, 76 (1960).